Electronic Supplementary Material (ESI) for Chemical Science

Supporting Information on

Homoconjugation in Diporphyrins: Excitonic Behaviors in Singly and Doubly Linked Zn(II)porphyrin Dimers

Min-Chul Yoon,[a] *Sangsu Lee,*[a] *Sumito Tokuji,*[b] *Hideki Yorimitsu,*[b] *Atsuhiro Osuka**[b] *and Dongho Kim**[a]

[a] Spectroscopy Laboratory for Functional π-Electronic Systems and Department of Chemistry, Yonsei University, Seoul 120-749, Korea. Fax: 82-2-2123-2436; Tel: 82-2-2123-2652; E-mail: dongho@yonsei.ac.kr

[b] Department of Chemistry and Graduate School of Science, Kyoto University, Sakyo-ku, Kyoto 606-8502, Japan. Fax: 81-75-753-3970; Tel: 81-75-753-4008; E-mail: osuka@kuchem.kyoto-u.ac.jp

S1. Experimental Details

Sample Preparation. The details in synthesis, characterization, and X-ray crystallographic analysis of SLZn and DLZn are described elsewhere.[1] The single crystals of SLZn and DLZn for X-ray analyses were obtained by the vapor diffusion method with dichloroethane/methanol and ethyl acetate/acetonitrile, respectively. ZnTPP (with low chlorine) and toluene (HPLC grade) were purchased from Aldrich and used without further purification.

Steady-State Absorption and Emission. Steady-state UV-vis absorption spectra were recorded on a commercial spectrometer (Cary5000, Varian). Fluorescence spectra were measured by a spectrophotometer (FL2500, Hitachi) and spectral sensitivity were corrected with the comparison of the well-known chromophores such as rhodamine and coumarin dyes.[2] For the steady-state fluorescence excitation anisotropy measurement, Glan laser and sheet polarizers were added into the excitation and monitoring paths, respectively. The calculation of anisotropy at specific monitoring wavelength (λ_{em}) as a function of excitation wavelength (λ_{ex}) was the given by

$$r(\lambda_{ex}) = [\, I_{VV}(\lambda_{ex}) - GI_{VH}(\lambda_{ex}) \,] / [\, I_{VV}(\lambda_{ex}) + 2GI_{VH}(\lambda_{ex}) \,] \quad (1)$$

where $I_{VV}(\lambda_{ex})$ (or $I_{VH}(\lambda_{ex})$) is the fluorescence intensity with the photoexcitation at λ_{ex} when the excitation light is vertically polarized and only the vertically (or horizontally) polarized portion of the fluorescence is detected, and the first and second subscripts represent excitation and detection polarizations, respectively. The factor of correction factor G is defined by $[\, I_{HV}(\lambda_{em}) / I_{HH}(\lambda_{em}) \,]$, which is equal to the ratio of the sensitivity of the detection system for vertically and horizontally polarized light at given emission wavelength λ_{em}. Experimental G value was measured to be around 1.7 in our instrument. All steady-state measurements were carried out by using a quartz cuvette with a pathlength of 1 cm at ambient temperatures.

Picosecond Time-resolved Emission. Time-resolved fluorescence decays were obtained by using a time-correlated single-photon counting (TCSPC) technique. A mode-locked Ti:sapphire oscillator (MaiTai-BB, Spectra Physics) were used as a excitation light source, which provide a fwhm (full width at half maximun) of 80 fs with a high repetition rate of 80 MHz. In order to minimize artifacts such as thermal lensing and accumulation effect, repetition rate was reduced down to 800 kHz using a home-made acousto-optic pulse selector. The picked fundamental pulses were frequency doubled by a 1 mm of thickness of BBO nonlinear crystal (Eksma). The fluorescence was collected by a microchannel plate photomultiplier (MCP-PMT, R3809U-51, Hamamatsu) with a thermoelectric cooler (C4878, Hamamatsu). Time-resolved fluorescence signals were calculated by a TCSPC board (SPC-130, Becker & Hickel GmbH). The overall instrumental response function (IRF) was determined to be less than 30 ps

(fwhm) in all spectral regions. A polarization of photoexcitation pulses was set to vertical to the laboratory frame by both a half-wave retarder and Glan laser polarizer and sheet polarizers were used in fluorescence collection path at magic angle (54.7°) to obtain polarization independent population decays. Time-resolved fluorescence anisotropy was obtained by changing the detection polarization on the fluorescence path to parallel or perpendicular to the polarization of the excitation pulses. The calculation of anisotropy decay at specific monitoring wavelength was the followed by

$$r(t) = [\ I_{VV}(t) - GI_{VH}(t)\ ] / [\ I_{VV}(t) + 2GI_{VH}(t)\ ] \quad (2)$$

where $I_{VV}(t)$ (or $I_{VH}(t)$) is the fluorescence decay when the excitation light is vertically polarized and only the vertically (or horizontally) polarized portion of the fluorescence is detected, and the first and second subscripts represent excitation and detection polarizations, respectively. The factor of correction factor G is defined by [$I_{HV}(t)$ / $I_{HH}(t)$], which is equal to the ratio of the sensitivity of the detection system for vertically and horizontally polarized light at specific monitoring wavelength. Experimental G values were measured to be around 1.12 in our instrument.

Femtosecond Time-resolved Emission. We used a femtosecond fluorescence up-conversion techniques to obtain fluorescence decay profiles for B-state of ZnTPP.[3] A home-built cavity-dumped mode-locked Ti:sapphire oscillator pumped by cw Nd:YVO4 (532 nm, Verdi V, Coherent) were used as a light source with a typical repetition rate of 200 kHz. The fundamental output pulses (center wavelength of 820 nm with spectral width of 80 nm) were compressed by fused silica prism pair and then frequency-doubled by 100 μm thick BBO. The second harmonic pulses around 410 nm and residual fundamental pulses were recompressed by another prism pairs and used as pump and gate pulses, respectively. Pump beam was focused to quartz cuvette (a 500 μm of thickness) containing sample solution by plano-convex lens with a focal length of 5 cm. The cuvette was continuously moved back and forth to minimize photodegradation of samples. Photo-induced fluorescence was collected and refocused on to the BBO crystal by reflected objective mirror (Coherent). The gate pulses was focused on to the same BBO and overlapped with fluorescence pulses by plano-convex lens with a focal length of 20 cm. Up-converted photons (sum-frequency generation between fluorescence and gate photons) were propagated into a monochromator (focal length of 30 cm, Dongwoo Optron) and detected by PMT (R3234-01, Hamamatsu). An electronic preamplifier, discriminator (C6465, Hamamatsu), and counter (PCI-6601, National Instruments) were used for the analogue-to-digital converting (ADC) for data acquisition and storage into a PC. Two sets of half-wave retarder and a Glan laser polarizers were used to control polarization of pump and gate pulse, respectively, for femtosecond time-resolved fluorescence anisotropy decay measurements. Same equation as used in ps time-resolved fluorescence anisotropy measurement for anisotropy calculation with G value of unity. The overall instrumental response function (IRF) was

determined to be 103 fs (fwhm) assuming Gaussian function.

Femtosecond Transient Absorption. Dual-beam femtosecond time-resolved transient absorption (TA) spectrometer consisted of two independently-tunable home-made optical parametric amplifiers (OPA) pumped by a regeneratively amplified Ti:sapphire laser system (Hurricane-X, Spectra-Physics) operating at 3 kHz repetition rate and an optical detection system.[4] The OPA was based on non-collinearly phase-matching geometry, which was easily color-tuned by controlling optical delay between white light continuum seed pulses (450-1400 nm) and visible pump pulses (400 nm) produced by using sapphire window and BBO crystal, respectively. The generated visible OPA pulses had a pulse width of ~ 35 fs and an average power of 5 mW at 3 kHz repetition rate in the range 500-700 nm after fused-silica prism compressor. Two OPA pulses were used as the pump and probe pulses, respectively, for TA measurement. The probe beam was split into two parts. The one part of the probe beam was overlapped with the pump beam at the sample to monitor the transient (signal), while the other part of the probe beam was passed through the sample without overlapping the pump beam to compensate the fluctuation of probe beam. The time delay between pump and probe beams was carefully controlled by making the pump beam travel along a variable optical delay (ILS250, Newport). To obtain the time-resolved transient absorption difference signal at specific wavelength, the monitoring wavelength was selected by using a narrow interference filter (FWHM ~10 nm). By chopping every another pump pulses at 1.5 kHz, the modulated probe pulses as well as the reference pulses were detected by two separate photodiodes (Femtowatt Photoreceiver, New Focus). The modulated signals of the probe pulses were measured by a gated-integrator (SR250, SRS) and a lock-in amplifier (DSP7265, EG&G) and stored in a personal computer for further signal processing. The polarization angle between pump and probe beam was set to magic angle (54.7°) in order to prevent polarization-dependent signals. In general experimental conditions, time-resolutions of less than 60 fs were achieved. For time-resolve transient absorption anisotropy (TAA) measurement, both $I_{//}(t)$ and $I_{\perp}(t)$ signals were collected simultaneously by combination of polarizing beam-splitter cube and dual lock-in amplifiers as following equation;

$$r(t) = [\, I_{//}(t) - I_{\perp}(t) \,] / [\, I_{//} + 2I_{\perp}(t) \,] \qquad (3)$$

where $I_{//}(t)$ and $I_{\perp}(t)$ represent TA signals with the polarization of the pump and probe pulses being mutually parallel and perpendicular respectively. This equation was also applied to the femtosecond fluorescence anisotropy measurement. The pump pulse was set to vertical polarization and that of probe pulse was set to 45° with respect to the pump pulse by using Glan-laser polarizers and half-wave plates. After the probe pulse passes through the sample cell, it was split by polarizing beam-splitter cube and then detected by two separate photodiodes. Two gated-integrators and two lock-in amplifiers record the

signal simultaneously within a single scan. As a standard anisotropy measurement showed a clean single exponential decay with reorientational relaxation times of 122.1 ± 0.3 ps and the initial anisotropy r_0 value of 0.39 ± 0.02 for rhodamine 6G dye in methanol, which are well-matched in other reference.[5] For all TA and TAA measurements, thin absorption cell with a pathlength of 500 μm was used to elimination of additional chirp.

Nonlinear Fitting for Anisotropy. For all ps and fs time-resolved fluorescence and transient absorption spectroscopies, anisotropy decay can be generally calculated by using experimentally measured decay profiles, $I_{//}$ and $I_{\perp}(t)$;

$$r(t) = [\, I_{//}(t) - GI_{\perp}(t) \,] / [\, I_{//} + 2GI_{\perp}(t) \,] \tag{4}$$

where, $I_{//}(t)$ and $I_{\perp}(t)$ correspond to signal intensities when the polarizations of probe pulses (or fluorescence pulses for emission decay) are parallel and perpendicular to those of pump pulses in TA spectroscopy. Ideally, correction factor G is unity for fs fluorescence up-conversion and TA anisotropy measurement whereas G is slightly higher than unity in typical spectrometer-based TCSPC anisotropy. And polarization independent population decay can be expressed by;

$$I_{mag}(t) = [\, I_{//}(t) + 2GI_{\perp}(t) \,] / 3 \tag{5}$$

In general, transition dipole moment of excited-state exponentially depolarized by vibrational dephasing, excitation energy transfer, rotational reorientation, etc.

$$r_{dep}(t) = \Sigma_i \,[\, c_i \cdot \exp(-t/\tau_{Ri}) \,] + r_{inf} \tag{6}$$

However, the measured anisotropy decay r(t) cannot be directly fit by eq 6 because non-impulsive excitation pulses give rise to broadened rise signals in zero-time region. Deconvolution fitting with IRF including a series of exponential functions should be done. In addition, $I_{//}(t)$ and $I_{\perp}(t)$ can be rewritten by using the relationship between anisotropy decays (eq 4) and population decay (eq 5);

$$I_{//}(t) = I_{mag} \cdot [\, 1 + 2r_{dep}(t) \,], \qquad I_{\perp}(t) = I_{mag} \cdot [\, 1 - 2r_{dep}(t) \,] \tag{7}$$

$$I_{diff} = I_{//}(t) - I_{\perp}(t) = 3I_{mag} \cdot r_{dep}(t) \tag{8}$$

The population decay can be regarded by convolution among at least three kinds of functions mathematically;

$$I_{mag}(t) = g(t) \otimes [\ s(t) \cdot \quad \Sigma_i\ (c_i \cdot \exp(-t/t_i))\ ] \tag{9}$$

where g(t) is instrumental response function, s(t) is step function, and third part is a series of exponential decay functions with amplitudes c_i and time constants t_i. We can obtain all parameters for population decay in eq 9 by least-square nonlinear fitting of experimental data $I_{mag}(t)$. Then, all parameters for anisotropy decay can be determined by least-square fitting of I_{diff} by using eq 8 with the fixed parameters related to the population decay. These deconvolution fitting procedure were applied for the analyses on all of our time-resolved anisotropy data.

S2. Theoretical Calculations

Quantum mechanical calculations were performed by the Gaussian03 program suite installed on supercomputer (KISTI).[6] Geometry optimizations were carried out by the density functional theory (DFT) method with the Becke's three-parameter hybrid exchange functional and the Lee-Yang-Parr correlation functional (B3LYP),[7, 8] employing a basis set containing 6-31G(d) for all atoms.[9] The X-ray crystallographic structures were used as initial geometries for geometry optimization.[1] To simulate the ground-state absorption spectra, we used time-dependent (TD) DFT calculations with the same functional and basis set as used in the geometry optimization.[10] Electron density difference maps (EDDM) were calculated by GAUSSSUM 2.2 program package using results of TDDFT.[11] All computational analyses were carried out omitting tertiary-butyl substituents in all phenyl groups to reduce computational cost since substituent effects on electronic structures of porphyrin rings by additional substituents far from porphyrin skeleton usually negligible in these systems.[12]

S3. References

1. S. Tokuji, C. Maeda, H. Yorimitsu and A. Osuka, *Chem. –Eur. J.*, 2011, **17**, 7154-7157.
2. J. Lakowicz, *Principles of Fluorescence Spectroscopy*, Kluwer Academic/Plenum Publishers, New York, Boston, Dordrecht, London, Moscow, 1999.
3. M. C. Yoon, D. H. Jeong, S. Cho, D. Kim, H. Rhee and T. Joo, *J. Chem. Phys.*, 2003, **118**, 164-171.
4. M. C. Yoon, S. Cho, P. Kim, T. Hori, N. Aratani, A. Osuka and D. Kim, *J. Phys. Chem. B*, 2009, **113**, 15074-15082.
5. L. A. Philips, S. P. Webb, S. W. Yeh and J. H. Clark, *J. Phys. Chem.*, 1985, **89**, 17-19.
6. M. J. Frisch, G. W. Trucks, H. B. Schlegel, G. E. Scuseria, M. A. Robb, J. R. Cheeseman, V. G. Zakrzewski, J. A. J. Montgomery, R. E. Stratmann, J. C. Burant, S. Dapprich, J. M. Millam, A. D. Daniels, K. N. Kudin, M. C. Strain, O. Farkas, J. Tomasi, V. Barone, M. Cossi, R. Cammi, B. Mennucci, C. Pomelli, C. Adamo, S. Clifford, J. Ochterski, G. A. Petersson, P. Y. Ayala, Q. Cui, K. Morokuma, D. K. Malick, A. D. Rabuck, K. Raghavachari, J. B. Foresman, J. Cioslowski, J. V. Ortiz, B. B. Stefanov, G. Liu, A. Liashenko, P. Piskorz, I. Komaromi, R. Gomperts, R. L. Martin, D. J. Fox, T. Keith, M. A. Al-Laham, C. Y. Peng, A. Nanayakkara, C. Gonzalez, M. Challacombe, P. M. W. Gill, B.

G. Johnson, W. Chen, M. W. Wong, J. L. Andres, M. Head-Gordon, E. S. Replogle and J. A. Pople, Gaussian, Inc., Wallingford CT, 2004.
7. A. D. Becke, *J. Chem. Phys.*, 1993, **98**, 5648-5652.
8. C. Lee, W. Yang and R. G. Parr, *Phys. Rev. B*, 1988, **37**, 785-789.
9. R. Ditchfield, W. J. Hehre and J. A. Pople, *J. Chem. Phys.*, 1971, **54**, 724-728.
10. R. Bauernschmitt and R. Ahlrichs, *Chem. Phys. Lett.*, 1996, **256**, 454-464.
11. N. M. O'Boyle, A. L. Tenderholt and K. M. Langner, *J. Comput. Chem.*, 2008, **29**, 839-845.
12. S. Cho, M.-C. Yoon, J. M. Lim, P. Kim, N. Aratani, Y. Nakamura, T. Ikeda, A. Osuka and D. Kim, *J. Phys. Chem. B*, 2009, **113**, 10619-10627.

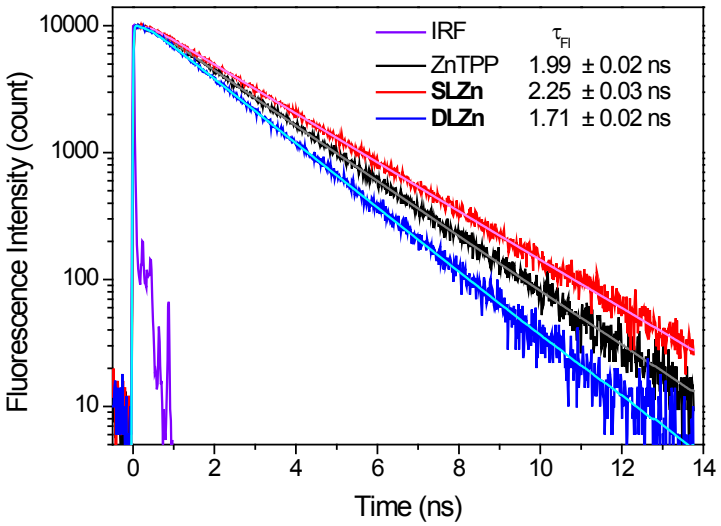

Fig. S1 Time-resolved fluorescence decay profiles of ZnTPP (black line), **SLZn** (red line) and **DLZn** (blue line) in toluene obtained by using TCSPC technique with the photoexcitation at 420 nm with the best fit curves (grey, pink, and cyan lines, respectively). Temporal profile for instrumental response function is plotted for the comparison (violet line, fwhm of ~ 30 ps).

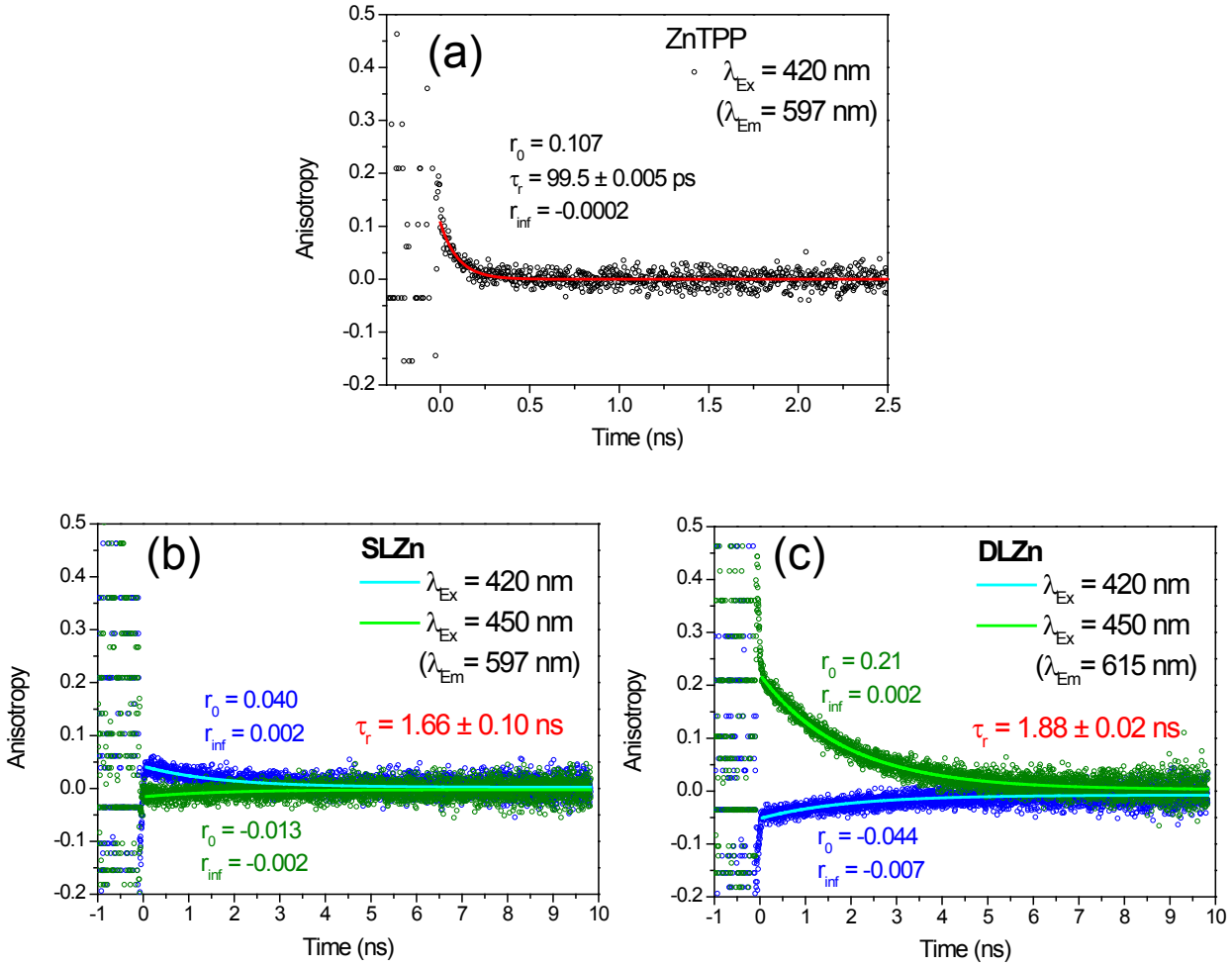

Fig. S2 Time-resolved fluorescence anisotropy decay profiles (open circles) of (a) ZnTPP, (b) **SLZn**, and (c) **DLZn** in toluene with the best fitting curves (solid lines). The various excitation and emission wavelengths were used and marked in legends. All data were fitted by using single exponential decay function with residual (r_{inf}). Determined decay time constants correspond to rotational reorientation times.

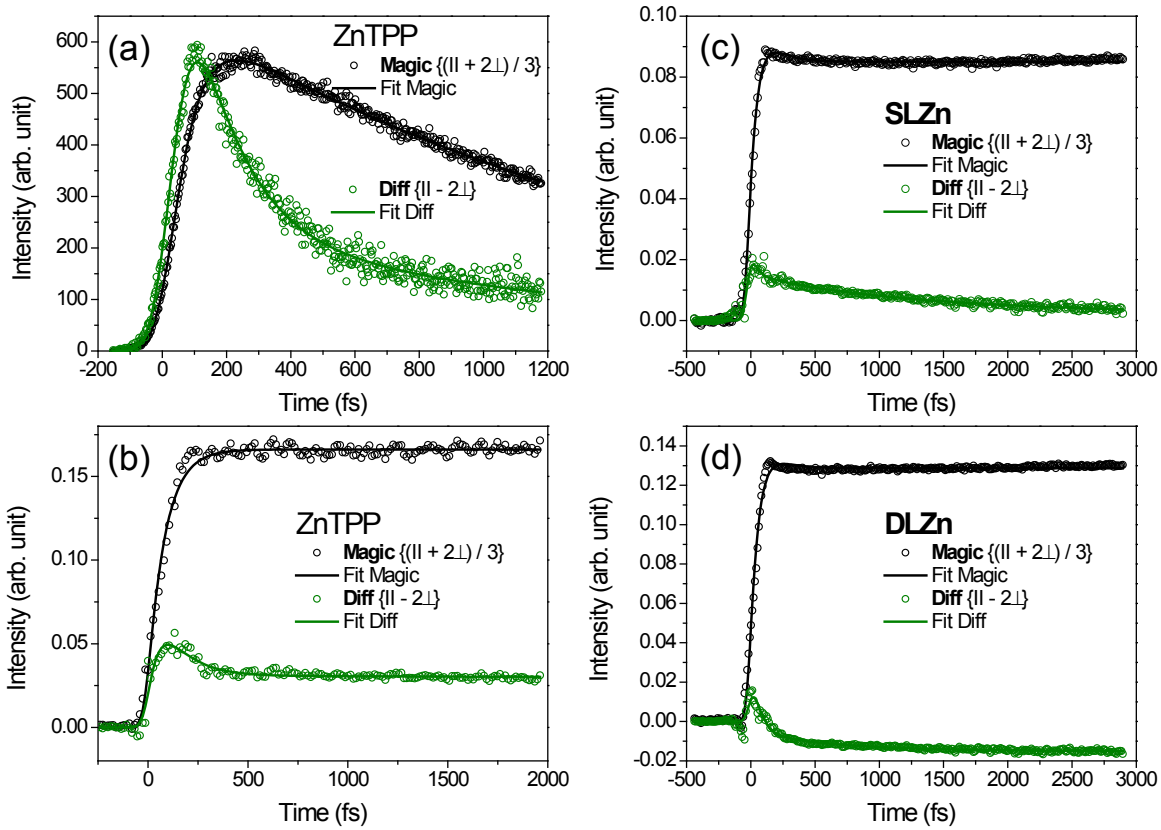

Fig. S3 Temporal profiles of population decay (black circles) and difference data between parallel and perpendicular signals (green circles) for (a) B-state and (b) Q-state of ZnTPP and Q-state of (c) **SLZn** and (d) **DLZn** measured by fluorescence up-conversion (a) and transient absorption (b-d), respectively. Solid lines correspond to the best fitting curves. Results of least-square fitting are listed in Table 2.

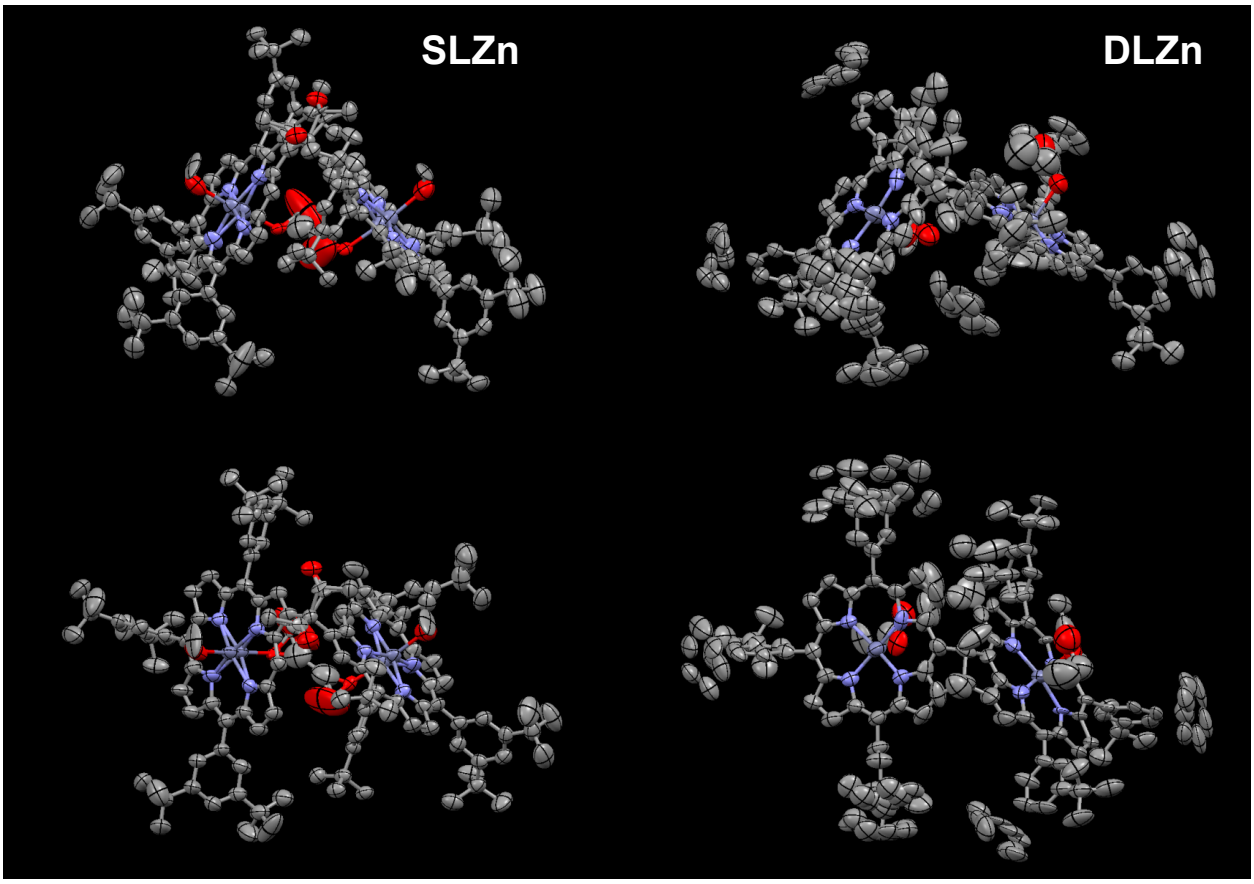

Fig. S4 (a) Side and (b) top view of X-ray crystallographic structures of **SLZn** and **DLZn** with a 30% probability level.

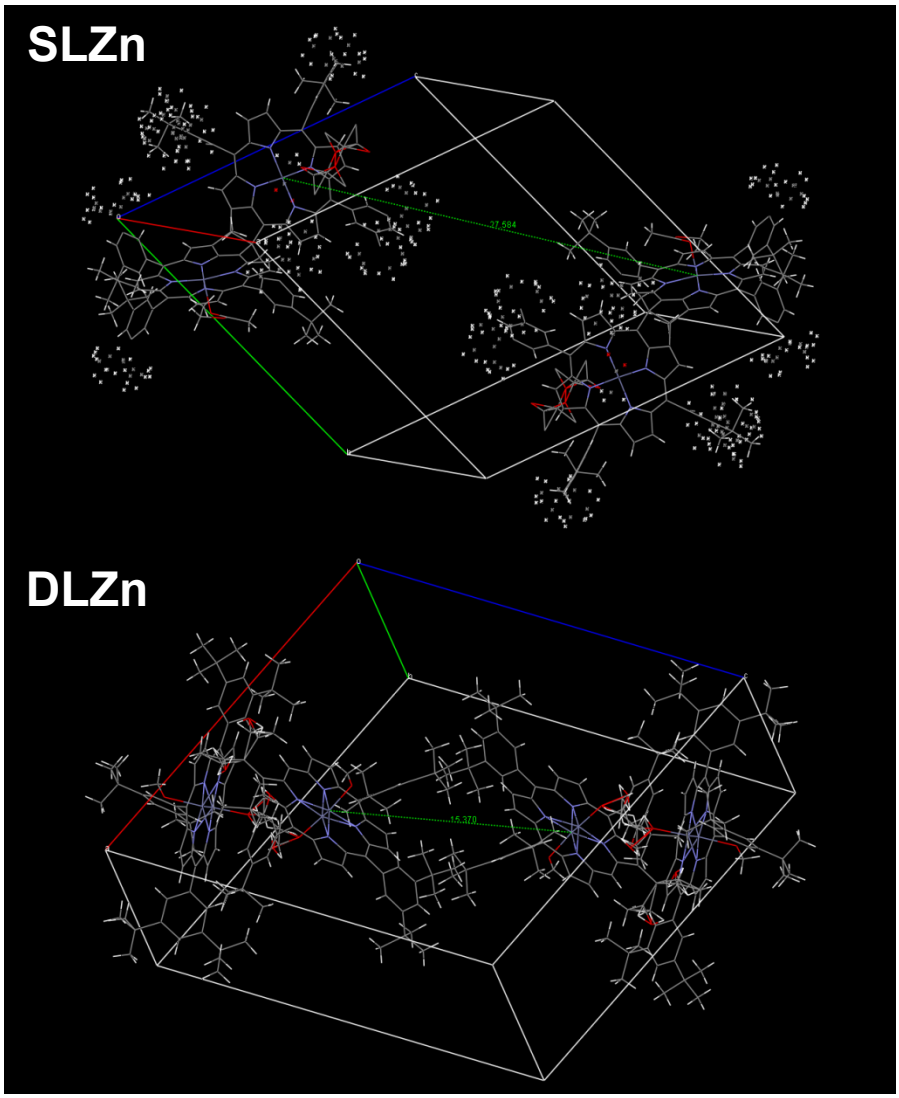

Fig. S5 Crystal packing structures of **SLZn** and **DLZn**. Distances between the nearest porphyrin pigments are measured to be 27.584 and 15.370 Å for **SLZn** and **DLZn**, respectively.

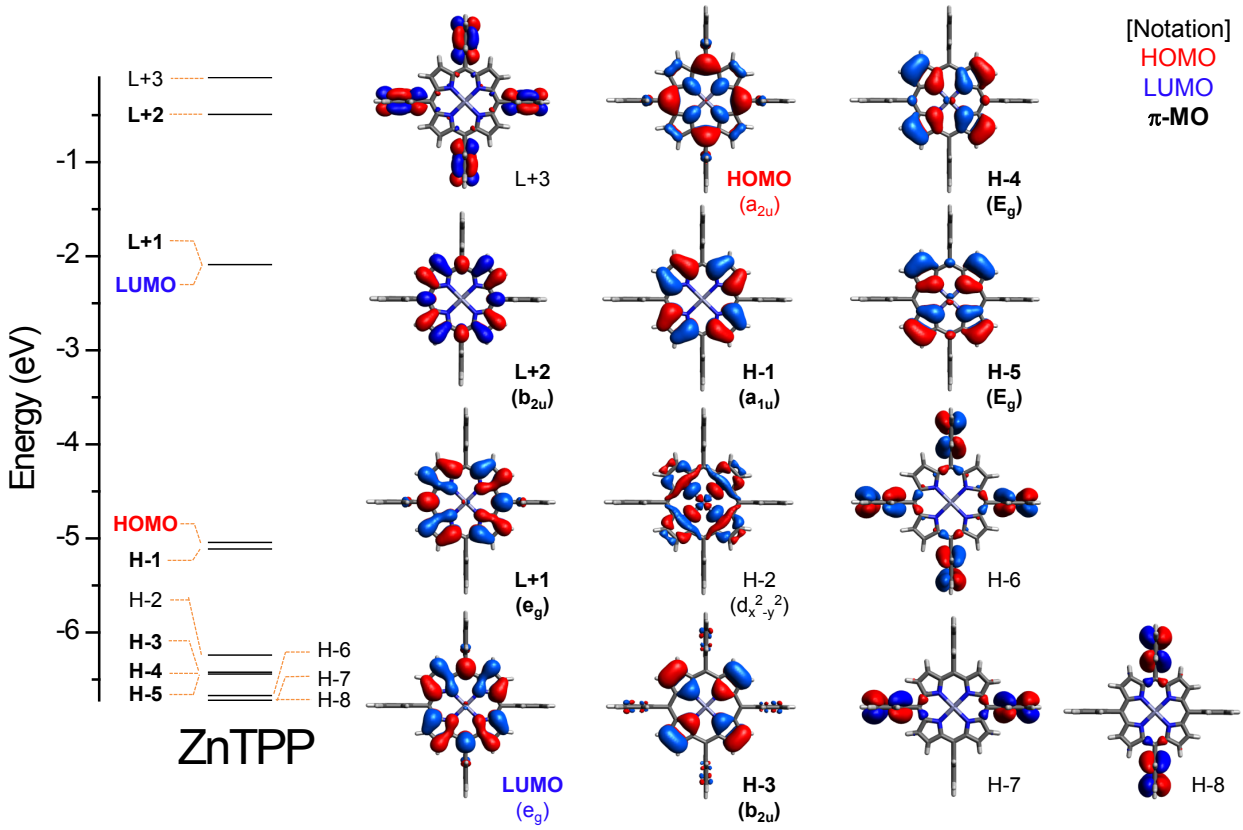

Fig. S6 Energy levels and structures of the frontier MOs of ZnTPP. In parentheses, all symmetries of MOs are denoted based on D_{4h} point group for each porphyrin moiety. Bold labels indicate π-MO of porphyrin moiety.

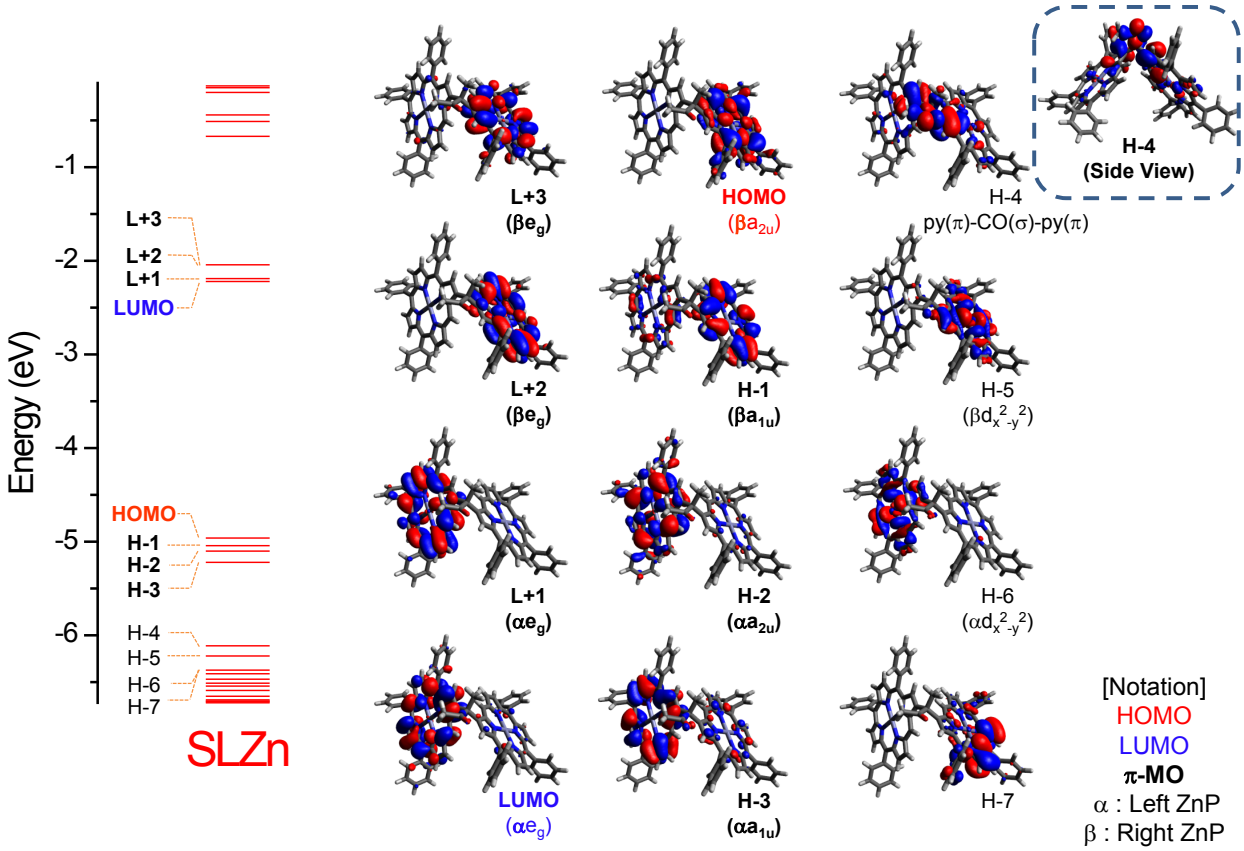

Fig. S7 Energy levels and structures of the frontier MOs of **SLZn**. In parentheses, all symmetries of MOs are denoted based on D_{4h} point group for each porphyrin moiety. Bold labels indicate π-MO of porphyrin moiety. α and β indicate Zn porphyrin moieties located in left- and right-side, respectively, in dimer systems.

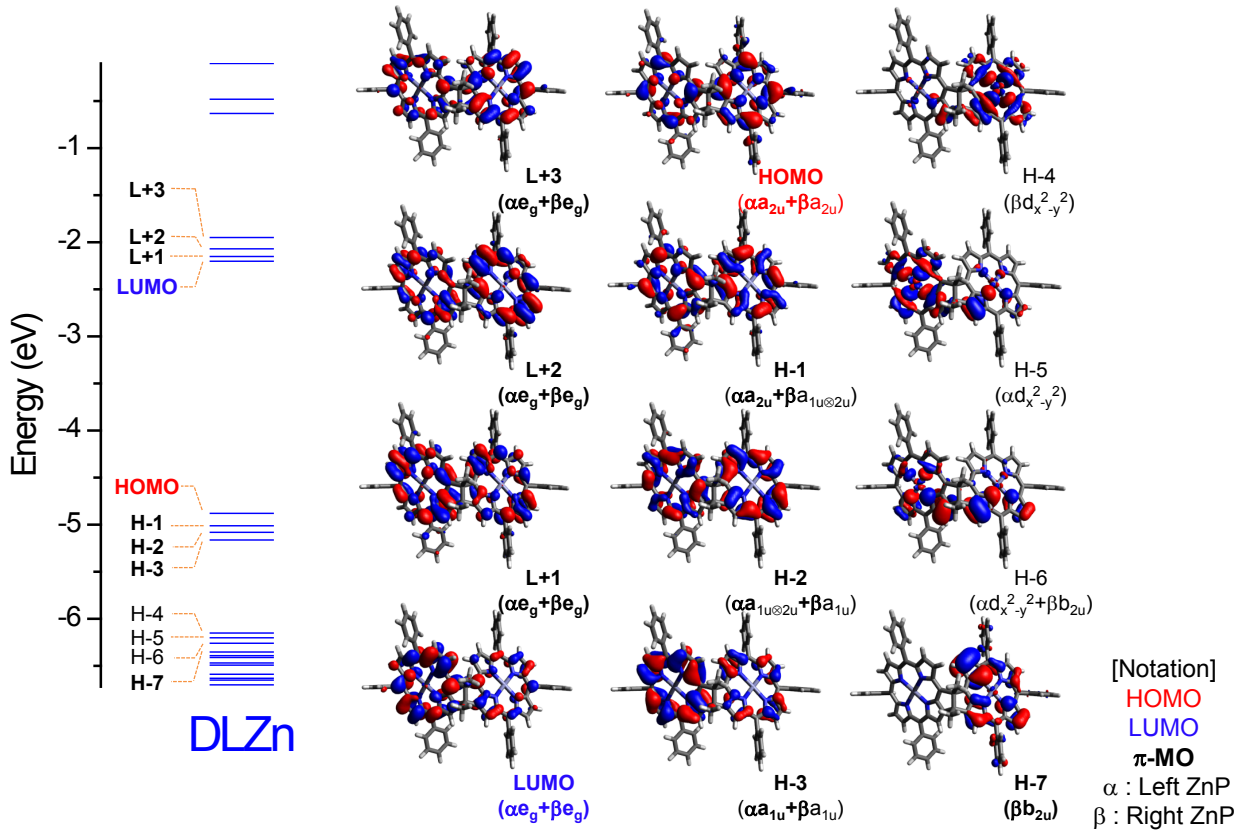

Fig. S8 Energy levels and structures of the frontier MOs of **DLZn**. In parentheses, all symmetries of MOs are denoted based on D_{4h} point group for each porphyrin moiety. Bold labels indicate π-MO of porphyrin moiety. α and β indicate Zn porphyrin moieties located in left- and right-side, respectively, in dimer systems.

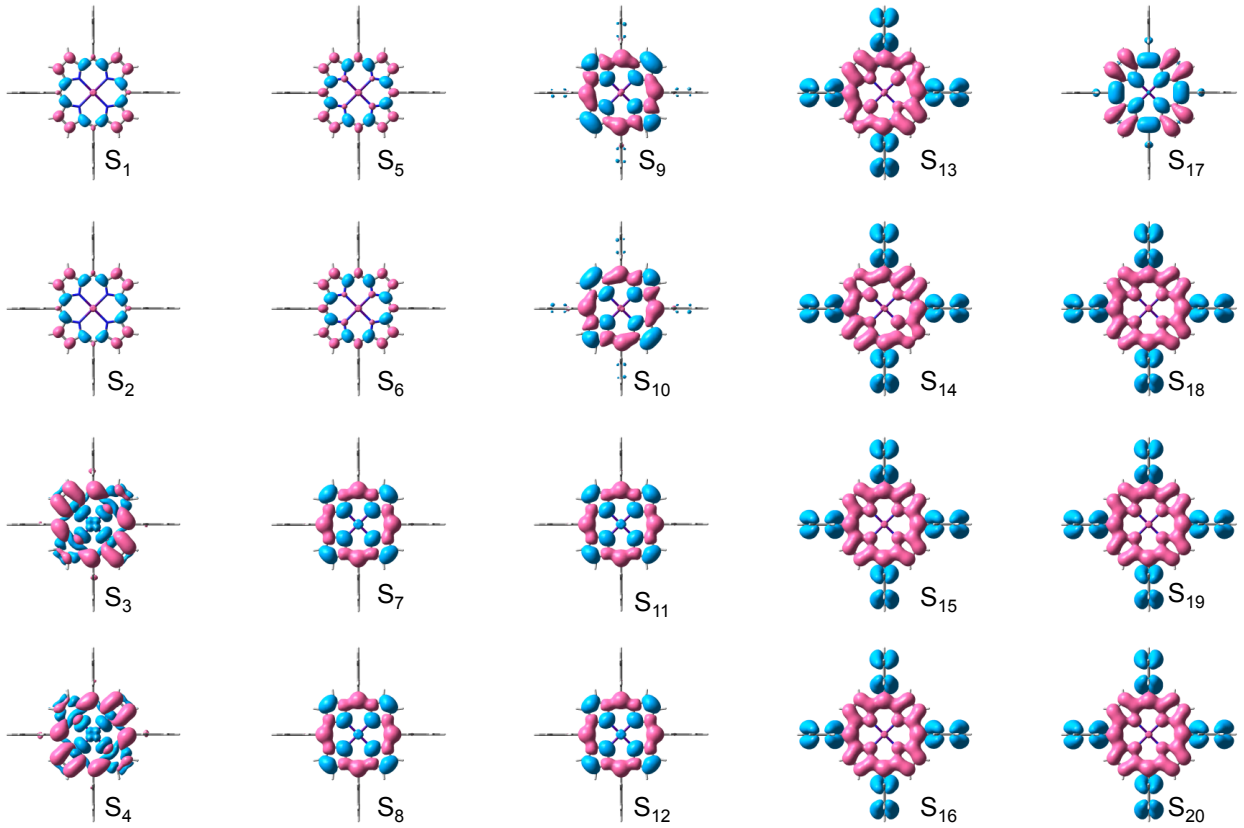

Fig. S9 Representative electron density difference maps between electronic ground and excited states of ZnTPP. Pink and blue colors indicate electron rich and deficient characters in excited electronic states.

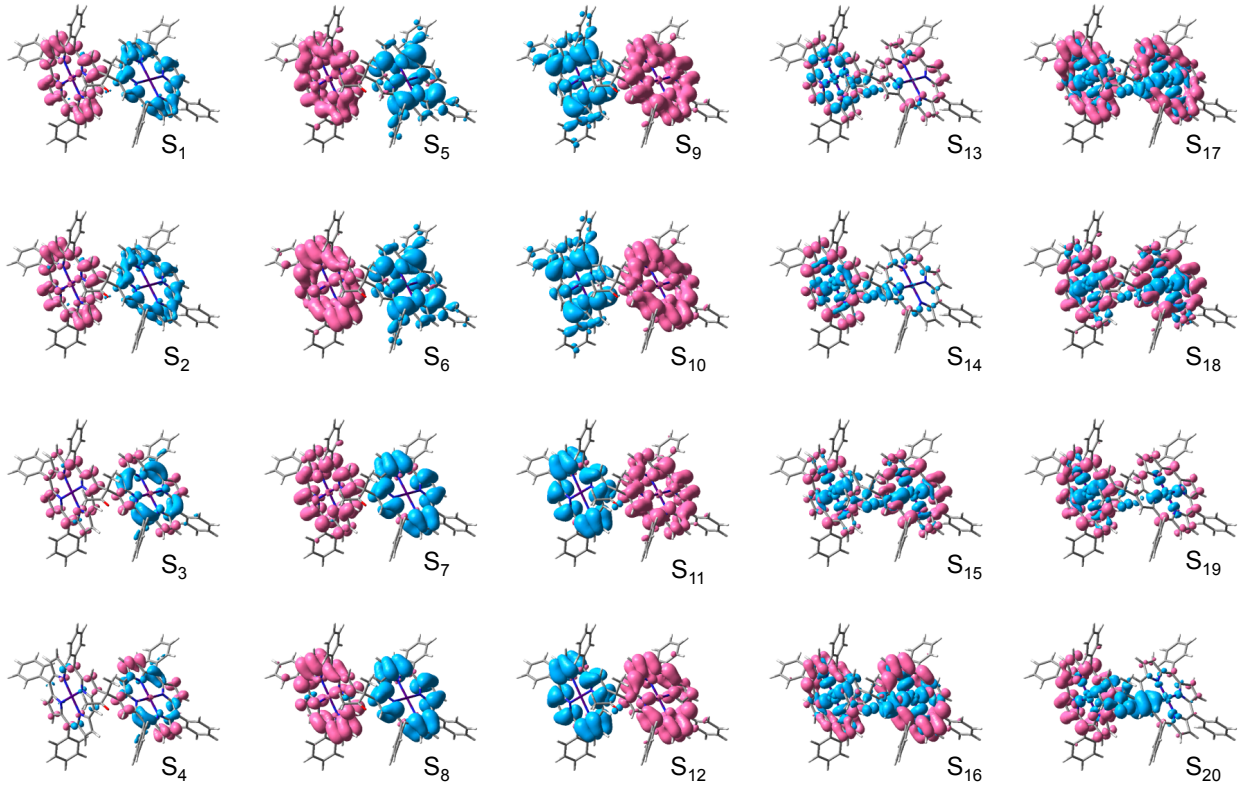

Fig. S10 Representative electron density difference maps between electronic ground and excited states of **SLZn**. Pink and blue colors indicate electron rich and deficient characters in excited electronic states.

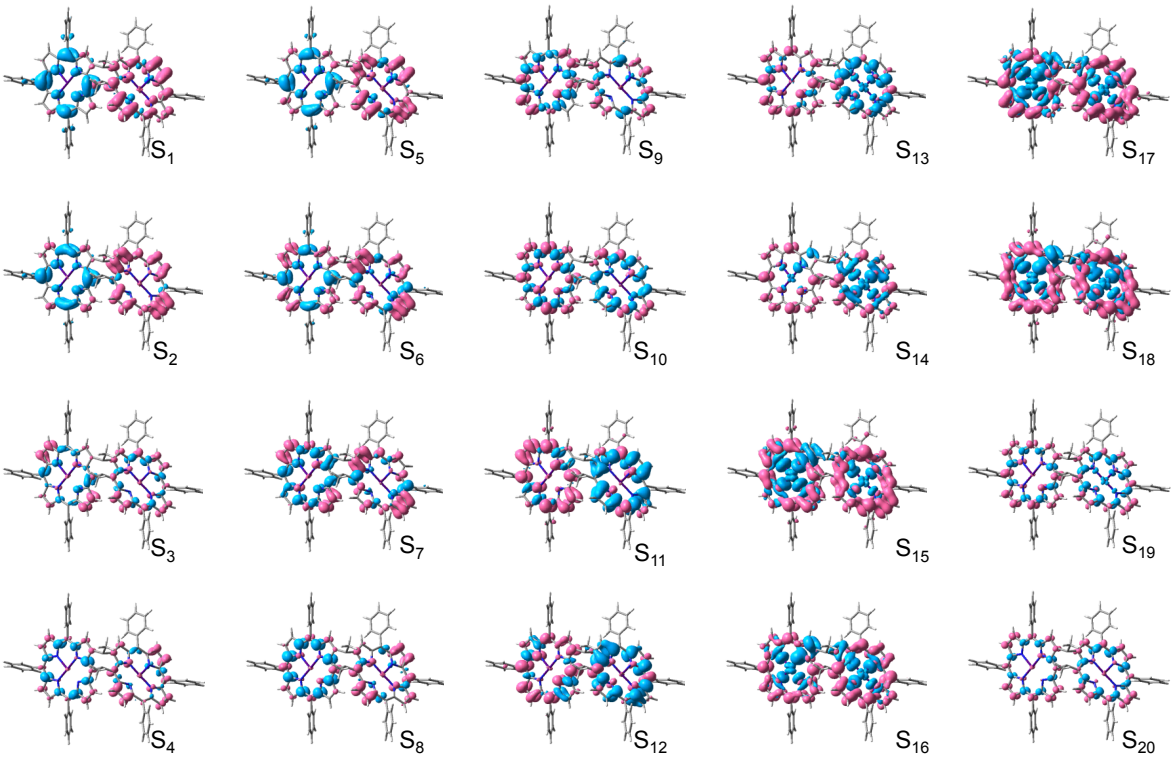

Fig. S11 Representative electron density difference maps between electronic ground and excited states of **DLZn**. Pink and blue colors indicate electron rich and deficient characters in excited electronic states.

Table S1 Calculated Vertical Excitation Energies of **ZnTPP** at B3LYP/6-31G(d) Level.

no	energy[a] [cm^{-1}]	energy[b] [eV]	λ[c] [nm]	f[d]	MO contribution[e]	nature[f]
1	19034	2.36	525.4	0.0013	H-1→LUMO (-15%), H-1→L+1 (-31%) HOMO→LUMO (35%), HOMO→L+1 (-18%)	π-π* (Q)
2	19034	2.36	525.4	0.0013	H-1→LUMO (31%), H-1→L+1 (-15%) HOMO→LUMO (18%), HOMO→L+1 (35%)	π-π* (Q)
3	26484	3.28	377.6	0	H-2→LUMO (95%)	MLCT
4	26485	3.28	377.6	0	H-2→L+1 (95%)	MLCT
5	27033	3.35	369.9	1.2964	H-1→LUMO (14%), H-1→L+1 (38%) HOMO→LUMO (32%), HOMO→L+1 (-12%)	π-π* (B)
6	27033	3.35	369.9	1.2964	H-1→LUMO (38%), H-1→L+1 (-14%) HOMO→LUMO (-12%), HOMO→L+1 (-32%)	π-π* (B)
7	29342	3.64	340.8	0	H-5→LUMO (28%), H-5→L+1 (-21%) H-4→LUMO (21%), H-4→L+1 (28%)	π_g-π_g*
8	29677	3.68	337.0	0	H-5→LUMO (15%), H-5→L+1 (34%) H-4→LUMO (34%), H-4→L+1 (-15%)	π_g-π_g*
9	30096	3.73	332.3	0.0593	H-3→LUMO (73%), H-3→L+1 (23%)	π_g-π_g*
10	30096	3.73	332.3	0.0593	H-3→LUMO (-23%), H-3→L+1 (73%)	π_g-π_g*
11	30657	3.80	326.2	0	H-5→LUMO (34%), H-5→L+1 (-15%) H-4→LUMO (-15%), H-4→L+1 (-34%)	π_g-π_g*
12	31356	3.89	318.9	0	H-5→LUMO (21%), H-5→L+1 (29%) H-4→LUMO (-29%), H-4→L+1 (21%)	π_g-π_g*
13	32379	4.01	308.8	0	H-6→LUMO (65%), H-6→L+1 (-21%)	CT (Ph-Por*)
14	32379	4.01	308.8	0	H-6→LUMO (21%), H-6→L+1 (65%)	CT (Ph-Por*)
15	32605	4.04	306.7	0	H-8→LUMO (17%), H-8→L+1 (32%) H-7→LUMO (32%), H-7→L+1 (-17%)	CT (Ph-Por*)
16	32623	4.05	306.5	0	H-8→LUMO (18%), H-8vL+1 (31%) H-7→LUMO (-31%), H-7→L+1 (18%)	CT (Ph-Por*)
17	32953	4.09	303.5	0	HOMO→L+2 (90%)	π_u-π_u*
18	33358	4.14	299.8	0.001	H-8→LUMO (31%), H-8→L+1 (-18%) H-7→LUMO (18%), H-7→L+1 (31%)	CT (Ph-Por*)
19	33395	4.14	299.4	0	H-8→LUMO (32%), H-8→L+1 (-18%) H-7→LUMO (-17%), H-7→L+1 (-32%)	CT (Ph-Por*)
20	33517	4.16	298.4	0	H-9→LUMO (51%), H-9→L+1 (36%) H-6→L+1 (-11%)	CT (Ph-Por*)

The calculated vertical excitation energies are expressed in wave number[a], electron Volt[b] and wavelength[c] scale. [d]Oscillator strength. [e]Minor configurations of which contributions are less than 10 % are omitted in list. [f]CT and MLCT indicate charge-transfer and metal-to-ligand charge transfer transition, respectively. Subscripts u and g correspond to character of inversion symmetry of involved each MO based on D_{4h} point group.

Table S2 Calculated Vertical Excitation Energies of **SLZn** at B3LYP/6-31G(d) Level.

no	energy[a] [cm^{-1}]	energy[b] [eV]	λ[c] [nm]	f[d]	MO contribution[e]	nature[f]
1	18615	2.31	537.2	0.0013	H-3→LUMO (15%), H-3→L+1 (-10%) H-2→LUMO (11%), H-2→L+1 (29%) H-1→LUMO (24%)	π_α-π_α* (Q_α) + π_β-π_α* (CT)
2	18689	2.32	535.1	0.0054	H-3→LUMO (-10%), H-3→L+1 (-18%) H-2→LUMO (32%), H-1→L+1 (-17%)	π_α-π_α* (Q_α) + π_β-π_α* (CT)
3	18796	2.33	532.0	0.0066	H-1→L+2 (33%), HOMO→LUMO (16%) HOMO→L+3 (34%)	π_β-π_β* (Q_β)
4	18831	2.33	531.0	0.0027	H-1→L+3 (-35%), HOMO→L+2 (43%)	π_β-π_β* (Q_β)
5	19386	2.40	515.8	0.0028	HOMO→LUMO (56%), HOMO→L+1 (22%)	π_β-π_α* (CT)
6	19632	2.43	509.4	0.0001	HOMO→LUMO (-14%), HOMO→L+1 (73%)	π_β-π_α* (CT)
7	20123	2.50	496.9	0.018	H-3→LUMO (-13%), H-1→LUMO (57%) H-1→L+1 (12%)	π_β-π_α* (CT)
8	20416	2.53	489.8	0.0145	H-3→L+1 (-13%), H-1→LUMO (-10%) H-1->L+1 (64%)	π_β-π_α* (CT)
9	21826	2.71	458.2	0.0049	H-2→L+2 (-34%), H-2→L+3 (58%)	π_α-π_β* (CT)
10	21912	2.72	456.4	0.0006	H-2→L+2 (59%), H-2→L+3 (32%)	π_α-π_β* (CT)
11	22572	2.80	443.0	0.0354	H-3→L+2 (-22%), H-3→L+3 (59%)	π_α-π_β* (CT)
12	22711	2.82	440.3	0.0369	H-3→L+2 (64%), H-3→L+3 (19%)	π_α-π_β* (CT)
13	25279	3.13	395.6	1.1939	H-3→LUMO (22%), H-3→L+3 (-13%) H-2→L+1 (-22%), HOMO→L+2 (12%)	π_α-π_α* (B_α)
14	25896	3.21	386.2	0.3979	H-6→LUMO (15%), H-3→L+1 (30%) H-2→LUMO (20%)	$MLCT_\alpha$ + π_α-π_α* (B_α)
15	26491	3.28	377.5	0.5134	H-6→L+1 (-10%), H-5→L+3 (23%) H-1→L+2 (17%), HOMO→L+3 (-15%)	$MLCT_\alpha$ + π_α-π_α* (B_α)
16	26628	3.30	375.5	0.0893	H-6→L+1 (-23%), H-5→L+2 (50%)	$MLCT_\alpha$+ $MLCT_\beta$
17	26721	3.31	374.2	0.1062	H-6→L+1 (34%), H-5→L+2 (24%) H-5→L+3 (16%)	$MLCT_\alpha$+ $MLCT_\beta$
18	26753	3.32	373.8	0.069	H-6→LUMO (34%), H-5→L+3 (32%)	$MLCT_\alpha$+ $MLCT_\beta$
19	27006	3.35	370.3	0.9585	H-6→LUMO (25%), H-1→L+2 (13%) HOMO→L+3 (-12%)	$MLCT_\alpha$ + π_β-π_β* (B_β)
20	27370	3.39	365.4	0.6665	H-4→LUMO (37%), H-1→L+3 (12%) HOMO→L+2 (12%)	CT_{bridge} + π-π* (B_β)

The calculated vertical excitation energies are expressed in wave number[a], electron Volt[b] and wavelength[c] scale. [d]Oscillator strength. [e]Minor configurations of which contributions are less than 10 % are omitted in list. [f]CT and MLCT indicate charge-transfer and metal-to-ligand charge transfer transition, respectively. Subscripts α and β represent two constituent monomeric units in dimer.

Table S3 Calculated Vertical Excitation Energies of **DLZn** at B3LYP/6-31G(d) Level.

no	energy[a] [cm^{-1}]	energy[b] [eV]	λ[c] [nm]	f[d]	MO contribution[e]	nature[f]
1	17943	2.22	557.3	0.0598	H-1→L+1 (-10%), HOMO→LUMO (61%)	π-π* (Q_α+Q_β)
2	18176	2.25	550.2	0.0062	H-2→LUMO (-14%), H-1→LUMO (16%) HOMO→L+1 (48%)	π-π* (Q_α+Q_β)
3	18575	2.30	538.4	0.0147	H-3→LUMO (-23%), HOMO→L+2 (35%)	π-π* (Q_α+Q_β)
4	18701	2.32	534.7	0.0042	H-3→L+1 (13%), H-2→L+2 (14%) H-1→LUMO (22%), HOMO-→+3 (-15%)	π-π* (Q_α+Q_β)
5	19828	2.46	504.3	0.0324	H-1→LUMO (13%), H-1→L+1 (23%) HOMO→LUMO (20%), HOMO→L+2 (-11%), HOMO→L+3 (13%)	π-π* (Q_α+Q_β)
6	20154	2.50	496.2	0.0001	H-1→LUMO (11%), H-1→L+2 (14%) HOMO→L+1 (-21%), HOMO→L+3 (24%)	π-π* (Q_α+Q_β)
7	20525	2.54	487.2	0.0127	H-2→LUMO (-10%), H-2→L+1 (14%) H-2→L+2 (12%), H-1→L+1 (10%) H-1→L+2 (21%), HOMO→L+2 (-17%)	π-π* (Q_α+Q_β)
8	20837	2.58	479.9	0.0107	H-3→LUMO (10%), H-2→LUMO (32%) H-2→L+1 (10%), H-1→L+2 (17%) H-1→L+3 (-12%)	π-π* (Q_α+Q_β)
9	21158	2.62	472.6	0.1851	H-2→L+3 (30%), H-1→LUMO (-10%) H-1→L+1 (10%), H-1→L+3 (11%)	π-π* (Q_α+Q_β)
10	21301	2.64	469.5	0.0194	H-3→L+1 (-14%), H-2→L+1 (-16%) H-2→L+2 (26%), H-1→L+3 (-22%)	π-π* (Q_α+Q_β)
11	21790	2.70	458.9	0.012	H-3→L+1 (22%), H-3→L+2 (53%)	π-π* (Q_α+Q_β)
12	22205	2.75	450.4	0.022	H-3→LUMO (-17%), H-3→L+3 (44%) H-2→L+3 (-12%)	π-π* (Q_α+Q_β)
13	25211	3.13	396.7	1.4626	H-3→L+2 (13%), H-3→L+3 (25%) H-2→L+3 (14%)	π-π* (B_α+B_β)
14	25668	3.18	389.6	0.5557	H-5→LUMO (18%)	MLCT + π_β-π_β* (B_β)
15	25882	3.21	386.4	0.0396	H-5→LUMO (-10%), H-4→L+1 (30%) H-4→L+2 (35%)	MLCT
16	25939	3.22	385.5	0.0589	H-6→LUMO (-11%), H-5→LUMO (27%) H-4→L+1 (13%), H-4→L+2 (11%)	MLCT
17	26279	3.26	380.5	0.0416	H-5→L+1 (-11%), H-4→LUMO (-29%) H-4→L+3 (32%)	MLCT
18	26308	3.26	380.1	0.1404	H-5→L+1 (30%), H-5→L+2 (-10%) H-4→LUMO (-13%)	MLCT
19	26940	3.34	371.2	1.97	H-3→LUMO (17%), H-2→L+3 (-16%) H-1→L+3 (12%), HOMO→L+2 (14%)	π-π* (B_α+B_β)
20	27403	3.40	364.9	0.6181	H-3→L+1 (21%), H-2→LUMO (-12%) H-1→L+2 (-16%), HOMO→L+3 (22%)	π-π* (B_α+B_β)

The calculated vertical excitation energies are expressed in wave number[a], electron Volt[b] and wavelength[c] scale. [d]Oscillator strength. [e]Minor configurations of which contributions are less than 10 % are omitted in list. [f]CT

and MLCT indicate charge-transfer and metal-to-ligand charge transfer transition, respectively. Subscripts α and β represent two constituent monomeric units in dimer.

Table S4 Full Cartesian Coordinates from Optimized Structures of All Compounds at B3LYP/6-31G(d) Level.

ZnTPP				
no.	atom	x	y	z
1	C	0.122395	-3.452702	-0.000021
2	C	-1.145252	-2.847711	-0.000017
3	C	1.344006	-2.759434	-0.000004
4	N	-1.390984	-1.493041	-0.000023
5	C	-2.396568	-3.570944	0.000031
6	N	1.493254	-1.390758	0.000017
7	C	2.643232	-3.392394	-0.000075
8	Zn	0.000019	-0.000503	-0.000019
9	C	-2.759527	-1.344029	0.000033
10	C	-3.392474	-2.643265	0.000009
11	H	-2.492349	-4.647369	0.000056
12	C	2.847800	-1.145272	0.000018
13	C	3.571025	-2.396594	-0.000070
14	H	2.814662	-4.459358	-0.000145
15	N	1.390712	1.493199	-0.000032
16	N	-1.492997	1.390932	0.000002
17	C	-3.452838	-0.122259	0.000058
18	H	-4.459421	-2.814728	0.000019
19	C	3.452820	0.122537	0.000009
20	H	4.647435	-2.492409	-0.000139
21	C	2.759414	1.343965	-0.000010
22	C	1.145218	2.847749	-0.000022
23	C	-1.343974	2.759475	-0.000001
24	C	-2.847697	1.145216	0.000042
25	C	3.392378	2.643301	-0.000015
26	C	2.396618	3.571007	0.000020
27	C	-0.122401	3.452893	-0.000012
28	C	-2.643294	3.392453	0.000079
29	C	-3.570939	2.396635	0.000021
30	H	4.459346	2.814729	-0.000001
31	H	-4.647367	2.492416	0.000027
32	H	-2.814727	4.459411	0.000117
33	H	2.492403	4.647425	0.000046
34	C	-4.954030	-0.175659	0.000079
35	C	-5.668645	-0.201318	-1.206259
36	C	-5.668597	-0.201674	1.206441
37	C	-7.063722	-0.251797	-1.206792
38	H	-5.123864	-0.181475	-2.146364
39	C	-7.063672	-0.252153	1.207015
40	H	-5.123773	-0.182109	2.146527
41	C	-7.764897	-0.276954	0.000121
42	H	-7.601936	-0.271148	-2.150947
43	H	-7.601853	-0.271784	2.151183
44	H	-8.851005	-0.316113	0.000141
45	C	0.175733	-4.953907	-0.000061
46	C	0.202402	-5.668504	1.206265
47	C	0.200753	-5.668489	-1.206436
48	C	0.252776	-7.063582	1.206773
49	H	0.183398	-5.123703	2.146377
50	C	0.251131	-7.063564	-1.207031
51	H	0.180469	-5.123672	-2.146511
52	C	0.276862	-7.764778	-0.000149
53	H	0.272884	-7.601779	2.150922
54	H	0.269958	-7.601754	-2.151210
55	H	0.315957	-8.850887	-0.000187
56	C	4.954016	0.175812	-0.000012
57	C	5.668656	0.200764	1.206325
58	C	5.668558	0.202549	-1.206374
59	C	7.063741	0.251034	1.206859
60	H	5.123890	0.180494	2.146431
61	C	7.063640	0.252809	-1.206947
62	H	5.123711	0.183655	-2.146460
63	C	7.764896	0.276757	-0.000054
64	H	7.601977	0.269783	2.151013
65	H	7.601805	0.272933	-2.151114
66	H	8.851009	0.315780	-0.000073
67	C	-0.175737	4.954086	0.000020
68	C	-0.201392	5.668666	1.206382
69	C	-0.201758	5.668707	-1.206313
70	C	-0.251762	7.063750	1.206970
71	H	-0.181612	5.123850	2.146469
72	C	-0.252124	7.063788	-1.206838
73	H	-0.182255	5.123918	-2.146421
74	C	-0.276848	7.764970	0.000083
75	H	-0.271086	7.601935	2.151142
76	H	-0.271726	7.602010	-2.150983
77	H	-0.315935	8.851081	0.000103

SLZn				
no.	atom	x	y	z
1	C	-1.729833	-0.996219	2.070368
2	C	-1.208175	-0.378952	3.284383
3	C	-2.075044	0.637705	3.577416
4	H	-2.017720	1.335304	4.399493
5	C	-3.104682	0.652799	2.565739
6	C	-4.161675	1.578971	2.510750
7	C	-5.135123	1.621034	1.495349
8	C	-6.255518	2.532733	1.479929
9	H	-6.468355	3.272119	2.238164
10	C	-6.977719	2.259535	0.359739
11	H	-7.891078	2.733534	0.031386
12	C	-6.309100	1.175888	-0.322457
13	C	-6.765867	0.589807	-1.517673
14	C	-6.176188	-0.522482	-2.146779
15	C	-6.611767	-1.077822	-3.407474
16	H	-7.428050	-0.701566	-4.006407
17	C	-5.790148	-2.126246	-3.686098
18	H	-5.809470	-2.766827	-4.555608
19	C	-4.841507	-2.222255	-2.600625
20	C	-3.802297	-3.170868	-2.534166
21	C	-2.824315	-3.209978	-1.525317
22	C	-1.766101	-4.194281	-1.430022
23	H	-1.616436	-5.015713	-2.115460
24	C	-1.029755	-3.880335	-0.328885
25	H	-0.156775	-4.388473	0.060996
26	C	-1.638427	-2.715294	0.263454
27	C	-1.171937	-2.095999	1.421147
28	H	-0.266613	-2.512593	1.847670
29	C	0.027173	-0.799585	4.070238
30	C	-0.234346	-2.136262	4.851556
31	C	-1.667073	-2.583096	5.076251
32	H	-1.667959	-3.392240	5.809176
33	H	-2.106942	-2.938665	4.137820
34	H	-2.294781	-1.755342	5.422013
35	O	0.687546	-2.753263	5.348221
36	N	-2.728679	-2.325842	-0.474496
37	N	-5.192277	0.798212	0.391499
38	N	-2.873070	-0.352202	1.659668
39	N	-5.092767	-1.230776	-1.677721
40	Zn	-3.963809	-0.768159	-0.038417
41	C	1.753161	0.150052	2.267779
42	C	1.271388	-0.888953	3.179303
43	C	2.178039	-1.907161	3.079128
44	H	2.169568	-2.839444	3.617790
45	C	3.190031	-1.512007	2.129165
46	C	4.277353	-2.317647	1.744931
47	C	5.254026	-1.946271	0.802031
48	C	6.383129	-2.768024	0.431472
49	H	6.599650	-3.747342	0.832319
50	C	7.096266	-2.073532	-0.496006
51	H	7.999604	-2.382250	-1.001507
52	C	6.421317	-0.812023	-0.692628
53	C	6.853666	0.187149	-1.582950
54	C	6.207825	1.419001	-1.790890
55	C	6.662091	2.439941	-2.706394
56	H	7.540039	2.371068	-3.332118
57	C	5.778586	3.471905	-2.622034
58	H	5.794563	4.401249	-3.172450
59	C	4.784328	3.100375	-1.641463
60	C	3.692358	3.906759	-1.266450
61	C	2.713656	3.534345	-0.328612
62	C	1.605470	4.366012	0.091307
63	H	1.406140	5.365036	-0.268241
64	C	0.897706	3.650423	1.008515
65	H	0.003285	3.945012	1.543202
66	C	1.572055	2.385768	1.165138
67	C	1.146921	1.382996	2.034850
68	H	0.230798	1.592726	2.571317
69	N	2.672225	2.334980	0.346839
70	N	5.299856	-0.757184	0.107760
71	N	2.913079	-0.256562	1.649962
72	N	5.064845	1.843692	-1.152272
73	Zn	3.986652	0.790027	0.228647
74	C	0.323485	0.209137	5.224127
75	H	-0.515887	0.272026	5.926147
76	H	1.207146	-0.129244	5.769787
77	H	0.517881	1.208913	4.828002
78	C	-4.254420	2.596525	3.607112
79	C	-4.596430	2.217321	4.914677
80	C	-3.998263	3.952599	3.349657
81	C	-4.679075	3.165604	5.935263
82	H	-4.806702	1.172236	5.125279
83	C	-4.079407	4.901398	4.369773
84	H	-3.729925	4.258663	2.342151
85	C	-4.420042	4.510779	5.666119
86	H	-4.951164	2.853078	6.940086
87	H	-3.873157	5.945935	4.151309
88	H	-4.484091	5.249378	6.460619

89	C	4.400465	-3.672719	2.374469
90	C	4.732920	-3.810749	3.730786
91	C	4.182419	-4.834579	1.617280
92	C	4.843735	-5.073813	4.313451
93	H	4.906388	-2.920010	4.328020
94	C	4.293430	-6.097987	2.199117
95	H	3.920111	-4.740843	0.566891
96	C	4.624479	-6.221453	3.549710
97	H	5.102133	-5.159611	5.365536
98	H	4.116809	-6.985652	1.597098
99	H	4.709561	-7.204933	4.004177
100	C	8.099291	-0.082764	-2.374846
101	C	9.361396	-0.047367	-1.762782
102	C	8.026821	-0.376681	-3.744968
103	C	10.519336	-0.300123	-2.499905
104	H	9.430443	0.184017	-0.703348
105	C	9.184188	-0.629219	-4.482964
106	H	7.054539	-0.411332	-4.228833
107	C	10.434168	-0.591892	-3.862479
108	H	11.488454	-0.265245	-2.008968
109	H	9.107770	-0.858837	-5.542628
110	H	11.335597	-0.788774	-4.436704
111	C	3.563788	5.254063	-1.909764
112	C	4.480532	6.277897	-1.623984
113	C	2.521302	5.522209	-2.810739
114	C	4.358807	7.533140	-2.221427
115	H	5.288302	6.085150	-0.923371
116	C	2.399069	6.777125	-3.408858
117	H	1.808752	4.736262	-3.045468
118	C	3.317492	7.786890	-3.116077
119	H	5.076426	8.314141	-1.983738
120	H	1.587557	6.963509	-4.107550
121	H	3.222604	8.764267	-3.581688
122	C	-3.726277	-4.200248	-3.619824
123	C	-4.713082	-5.191330	-3.740123
124	C	-2.665756	-4.196247	-4.539717
125	C	-4.640423	-6.152226	-4.749411
126	H	-5.535796	-5.208412	-3.030674
127	C	-2.593616	-5.155764	-5.550262
128	H	-1.899735	-3.429624	-4.462670
129	C	-3.580459	-6.137346	-5.657919
130	H	-5.411124	-6.915113	-4.822694
131	H	-1.767420	-5.132980	-6.256076
132	H	-3.524143	-6.885294	-6.444287
133	C	-7.970588	1.196969	-2.170098

134	C	-9.184134	0.494543	-2.236467
135	C	-7.909621	2.482331	-2.731269
136	C	10.304484	1.061059	-2.845669
137	H	-9.246003	-0.498428	-1.799899
138	C	-9.028983	3.048687	-3.342217
139	H	-6.973985	3.033169	-2.692335
140	C	10.230241	2.339777	-3.401123
141	H	11.236802	0.503610	-2.882554
142	H	-8.960349	4.042861	-3.776075
143	H	11.102421	2.780648	-3.876429

DLZn				
no.	atom	x	y	z
1	C	-3.671486	-2.227318	-1.429952
2	C	-2.582796	-2.905553	-2.120856
3	H	-2.584212	-3.950688	-2.396035
4	C	-1.200982	0.309938	-1.813323
5	C	-1.468169	1.559614	-1.231970
6	C	-1.303604	3.683783	-0.494862
7	H	-0.964438	4.679327	-0.248250
8	C	-2.581426	3.118026	-0.124824
9	C	-3.578479	3.806809	0.595987
10	C	-4.812848	3.265414	1.002399
11	C	-5.853309	4.010546	1.671001
12	H	-5.800587	5.057470	1.931398
13	C	-6.891972	3.154846	1.877740
14	H	-7.843926	3.373818	2.338832
15	C	-6.503683	1.872654	1.339266
16	C	-7.324581	0.726764	1.342048
17	C	-6.989599	-0.511352	0.762565
18	C	-7.828232	-1.689620	0.774484
19	H	-8.805957	-1.757696	1.228974
20	C	-7.149804	-2.665984	0.111539
21	H	-7.477079	-3.676423	-0.086332
22	C	-5.881399	-2.102218	-0.298044
23	C	-4.887230	-2.801534	-1.016700
24	C	2.467024	-2.840407	-0.327921
25	C	2.313232	1.114823	-2.202581
26	C	-1.603683	-1.966957	-2.291092
27	C	-2.091429	-0.757671	-1.720827
28	C	-0.622531	2.724890	-1.181476
29	H	0.373892	2.801586	-1.586012
30	C	1.289025	-3.293120	-1.055507
31	H	0.910521	-4.305347	-1.048654
32	C	0.823417	-2.201429	-1.734113
33	C	1.702250	-1.124771	-1.426787
34	C	2.243444	2.307567	-3.014119
35	H	1.447153	2.569443	-3.693609
36	C	1.395761	0.055098	-2.106937
37	C	3.373753	3.027881	-2.770015
38	H	3.653967	3.977940	-3.201425
39	C	4.154874	2.281522	-1.810285
40	C	5.374339	2.727390	-1.261662
41	C	6.141768	2.034297	-0.308107
42	C	7.372404	2.523843	0.267811
43	H	7.832737	3.473574	0.037528
44	C	7.816256	1.573356	1.135723
45	H	8.704319	1.604905	1.749903
46	C	6.878990	0.475559	1.084140
47	C	7.014807	-0.725021	1.808308
48	C	6.139118	-1.824269	1.726339
49	C	6.308451	-3.076611	2.429161
50	H	7.111911	-3.306322	3.114055
51	C	5.276362	-3.882891	2.056404
52	H	5.073110	-4.889601	2.391680
53	C	4.467377	-3.134878	1.118168
54	C	3.288872	-3.619097	0.506590
55	C	-0.011614	-0.137971	-2.725757
56	C	-0.194435	-1.775107	-2.764640
57	C	0.110283	-2.428738	-4.124197
58	H	-0.597598	-2.109972	-4.895159
59	H	0.035707	-3.517436	-4.027602
60	H	1.126765	-2.193782	-4.456818
61	C	-0.220578	0.496230	-4.114835
62	H	-0.331543	1.580583	-4.037017
63	H	-1.146186	0.118310	-4.560845
64	H	0.609905	0.277561	-4.793664
65	N	3.503102	1.115417	-1.491957
66	N	-5.813327	-0.787956	0.107970
67	N	-5.235897	1.967826	0.804964
68	N	2.700586	-1.503771	-0.596593
69	N	5.860819	0.787135	0.207732
70	N	-3.330202	-0.909426	-1.193074
71	N	5.014607	-1.884471	0.939541
72	N	-2.659058	1.821587	-0.572618
73	Zn	-4.268018	0.543179	-0.206050
74	Zn	4.263254	-0.338240	-0.197139
75	C	-5.131906	-4.239037	-1.352886
76	C	-5.270182	-4.650750	-2.688159
77	C	-5.220014	-5.210196	-0.342443
78	C	-5.491311	-5.991878	-3.003723
79	H	-5.211826	-3.908634	-3.479503
80	C	-5.441277	-6.551320	-0.657249
81	H	-5.105920	-4.906926	0.694533
82	C	-5.577675	-6.946971	-1.989189
83	H	-5.601394	-6.289076	-4.043450
84	H	-5.502120	-7.288150	0.139529
85	H	-5.750097	-7.991519	-2.234569
86	C	-8.662528	0.838719	2.009489
87	C	-8.759759	0.958159	3.404594
88	C	-9.845787	0.825128	1.254757

89	C	10.004338	1.059608	4.027563
90	H	-7.850903	0.964840	3.999980
91	C	11.090855	0.927614	1.876819
92	H	-9.783313	0.740350	0.173356
93	C	11.173986	1.044917	3.265462
94	H	10.059400	1.146492	5.109631
95	H	11.995806	0.919880	1.274796
96	H	12.143344	1.124539	3.750315
97	C	-3.306189	5.237238	0.953442
98	C	-3.247199	6.227381	-0.039802
99	C	-3.104573	5.617314	2.289539
100	C	-2.994452	7.558781	0.292892
101	H	-3.407190	5.946873	-1.077171
102	C	-2.850256	6.948287	2.623037
103	H	-3.141278	4.859237	3.066981
104	C	-2.794809	7.923568	1.625638
105	H	-2.957528	8.311690	-0.490178
106	H	-2.691244	7.221719	3.662921
107	H	-2.597279	8.960275	1.885022
108	C	5.890104	4.059019	-1.724196
109	C	6.471814	4.199379	-2.993183
110	C	5.800538	5.189914	-0.898598
111	C	6.951090	5.436953	-3.425563
112	H	6.550945	3.329383	-3.639480
113	C	6.280168	6.427716	-1.329818
114	H	5.347802	5.093960	0.084540
115	C	6.856985	6.554896	-2.594787
116	H	7.401361	5.525763	-4.410856
117	H	6.199493	7.293340	-0.677455
118	H	7.230390	7.518575	-2.930827
119	C	8.195759	-0.853272	2.724640
120	C	9.489046	-1.035431	2.211404
121	C	8.028027	-0.801699	4.116780
122	C	10.584989	-1.160459	3.066451
123	H	9.630243	-1.084280	1.135151
124	C	9.123504	-0.926465	4.972568
125	H	7.031546	-0.658459	4.525661
126	C	10.405460	-1.105958	4.449857
127	H	11.578816	-1.304439	2.650518
128	H	8.974428	-0.880493	6.048228
129	H	11.258606	-1.203355	5.115968
130	C	2.890387	-5.038082	0.757935
131	C	1.683524	-5.341974	1.408784
132	C	3.710608	-6.099702	0.341890
133	C	1.309661	-6.666393	1.638507

134	H	1.043145	-4.530747	1.743320
135	C	3.336274	-7.424050	0.570199
136	H	4.642189	-5.879150	-0.171673
137	C	2.134533	-7.712037	1.219882
138	H	0.374431	-6.880121	2.149338
139	H	3.982515	-8.231244	0.235196
140	H	1.842919	-8.743621	1.398270